

# Tensor Neural Network and Its Numerical Integration\*

Yifan Wang<sup>†</sup>, Pengzhan Jin<sup>‡</sup> and Hehu Xie<sup>§</sup>

## Abstract

In this paper, we introduce a type of tensor neural network. For the first time, we propose its numerical integration scheme and prove the computational complexity to be the polynomial scale of the dimension. Based on the tensor product structure, we design an efficient numerical integration method by using fixed quadrature points for the functions by the tensor neural network. The corresponding machine learning method is also introduced for solving high-dimensional eigenvalue problems. Some numerical examples are also provided to validate the theoretical results and the numerical algorithm.

**Keywords.** Tensor neural network, numerical integration, fixed quadrature points, high-dimensional eigenvalue problem.

**AMS subject classifications.** 65N30, 65N25, 65L15, 65B99

## 1 Introduction

Partial differential equations appear in many scientific and industrial applications since they can describe the physical and engineering phenomena or processes. So far, there have been developed many types of numerical methods such as finite difference method, finite element method, spectral method for solving PDEs in three spatial dimensions plus the temporal dimension. But there exist many high-dimensional PDEs such as many-body Schrödinger, Boltzmann equations, Fokker-Planck equations, stochastic PDEs (SPDEs), which are almost impossible solved by the traditional numerical methods. Recently, many numerical methods have been proposed based on the machine learning to solve the high-dimensional PDEs ([1, 4, 5, 13, 19, 20, 25]). Among these machine learning methods, neural network-based methods attract more and more attentions. The neural networks (NNs) can be used to build the approximation to the exact solution for the PDEs. The

---

\*This work was supported in part by the National Key Research and Development Program of China (2019YFA0709601), the National Center for Mathematics and Interdisciplinary Science, CAS.

<sup>†</sup>LSEC, NCMIS, Institute of Computational Mathematics, Academy of Mathematics and Systems Science, Chinese Academy of Sciences, Beijing 100190, China, and School of Mathematical Sciences, University of Chinese Academy of Sciences, Beijing 100049, China (wangyifan@lsec.cc.ac.cn).

<sup>‡</sup>School of Mathematical Sciences, Peking University, Beijing 100871, China (jpz@pku.edu.cn).

<sup>§</sup>LSEC, NCMIS, Institute of Computational Mathematics, Academy of Mathematics and Systems Science, Chinese Academy of Sciences, Beijing 100190, China, and School of Mathematical Sciences, University of Chinese Academy of Sciences, Beijing 100049, China (hhxie@lsec.cc.ac.cn).

reason is that NNs are able to approximate any function given enough parameters. This type of method provides a possible way to solve many useful high-dimensional PDEs from physics, chemistry, biology, engineers and so on.

Due to its universal approximation property, the fully-connected neural network (FNN) is the most widely used architecture to build the functions for solving high-dimensional PDEs. There are several types of FNN-based methods such as deep Ritz [4, 5], PINN [22] for solving high-dimensional PDEs by designing different loss functions. Among these methods, the loss functions always include computing high-dimensional integration for the functions defined by FNN. For example, the loss functions of the deep Ritz method require to compute the integrations on the high-dimensional domain for the functions which is constructed by FNN. Direct numerical integration for the high-dimensional functions also meet the “curse of dimensionality”. Always, Monte-Carlo method is adopted to do the high-dimensional integration with some types of sampling methods [5]. Due to the low convergence rate of Monte-Carlo method, the solutions obtained by the FNN-based numerical methods have only low accuracy and always have no stable convergence behaviors. Furthermore, the integration process with Monte Carlo method also need much computational work which decreases the simulation efficiency for the FNN-based numerical methods for solving high-dimensional PDEs. These considerations mean that the FNN-based method with Monte Carlo integrations also has the “curse of dimensionality” in some sense.

The CANDECOMP/PARAFAC (CP) tensor decomposition builds a low-rank approximation method and is a widely used way to cope with the curse of dimensionality. The CP method decomposes a tensor as a sum of rank-one tensors which can be considered as the higher-order extensions of the singular value decomposition (SVD) for the matrices. This means the SVD idea can be generalized to the decomposition of the high-dimensional Hilbert space into the tensor product of several Hilbert spaces. The tensor product decomposition has been used to establish low-rank approximations of operators and functions [3, 12, 15, 23]. If we use the low-rank approximation to do the numerical integration, the computational complexity can avoid the exponential dependence on the dimension in some cases [2, 20]. It is worth mentioning that although CP decomposition should be useful to obtain a low-rank approximation, there is no known general result to give the relationship between the rank and error bounds. For more details, please refer to [14, 17] and numerical investigations [3].

The aim of this paper is to propose a type of tensor neural network (TNN) to build the functions for solving high-dimensional PDEs. The TNN is a function being designed by the tensor product way or by low-rank CP decomposition structure. An important advantage is that we do not need to use Monte Carlo to do the integration for the functions which is constructed by TNN. This is the main motivation to design TNN in this paper. We will show, the computational work for the integration of the functions by TNN is only polynomial scale with respect to the dimension, which means the TNN overcomes the “curse of dimensionality” in some sense for solving high-dimensional PDEs.

An outline of the paper goes as follows. In Section 2, we introduce the way to build TNN. The numerical integration method for the functions constructed by TNN is designed in Section 3.

Section 4 is devoted to proposing the machine learning method for solving the high-dimensional eigenvalue problem with TNN and the numerical integration method. Some numerical examples are provided in Section 5 to show the validity and efficiency of the proposed numerical methods in this paper. Some concluding remarks are given in the last section.

## 2 Tensor neural network architecture

In the section, we introduce the TNN and its approximation property. The architecture of TNN is similar to MIONet, just by setting the Banach spaces to Euclidean spaces, more details can be found in [15]. More specifically, we first construct  $d$  subnetworks, where each subnetwork is a continuous mapping from a bounded closed set  $\Omega_i \subset \mathbb{R}$  to  $\mathbb{R}^p$ . The  $i$ -th subnetwork can be expressed as:

$$\phi_i(x_i; \theta_i) = (\phi_{i,1}(x_i; \theta_i), \phi_{i,2}(x_i; \theta_i), \dots, \phi_{i,p}(x_i; \theta_i))^T, \quad i = 1, \dots, d, \quad (1)$$

where  $x_i$  denotes the one-dimensional input,  $\theta_i$  denotes the parameters of the  $i$ -th subnetwork, typically the weights and biases. The number of layers and neurons in each layer, the selections of activation functions and other hyperparameters can be different in different subnetworks. In this paper, we simply use FNN architectures for each subnetwork. It is worth mentioning that, in addition to FNN, other reasonable architecture can be used as long as it can approximate any mapping from  $\Omega_i \subset \mathbb{R}$  to  $\mathbb{R}^p$  in some sense. The only thing to be guaranteed is that the output dimensions of these subnetworks should be equal. After identifying each subnetwork, we combine the output layers of each subnetwork to obtain TNN architecture by the following mapping from  $\mathbb{R}^d$  to  $\mathbb{R}^K$

$$\Psi(x; \theta) = W \cdot (\phi_1(x_1; \theta_1) \odot \phi_2(x_2; \theta_2) \odot \dots \odot \phi_d(x_d; \theta_d)),$$

where  $\odot$  is the Hadamard product (i.e., element-wise product), the matrix  $W \in \mathbb{R}^{K \times p}$  and  $x = (x_1, \dots, x_d) \in \Omega_1 \times \dots \times \Omega_d$ . In the following part of this paper, we set  $\Omega = \Omega_1 \times \dots \times \Omega_d$ . Note that here  $\theta = \{\theta_1, \dots, \theta_d, W\}$  are trainable parameters. Since it is sufficient to study the one-dimensional output case for the numerical integration on the tensor-product type domain  $\Omega$ , in this paper, without loss of generality, we only consider the case  $K = 1$  as follows:

$$\Psi(x; \theta) = \sum_{j=1}^p \phi_{1,j}(x_1; \theta_1) \phi_{2,j}(x_2; \theta_2) \dots \phi_{d,j}(x_d; \theta_d) = \sum_{j=1}^p \prod_{i=1}^d \phi_{i,j}(x_i; \theta_i), \quad (2)$$

where  $\theta = \{\theta_1, \dots, \theta_d\}$  denotes all the parameters of the whole architecture.

Since there exists the isomorphism relation between  $L^2(\Omega_1 \times \dots \times \Omega_d)$  and the tensor product space  $L^2(\Omega_1) \otimes \dots \otimes L^2(\Omega_d)$ , the process of approximating the function  $f(x) \in L^2(\Omega_1 \times \dots \times \Omega_d)$  with the TNN defined by (2) can be regarded as searching for a CP decomposition structure to approximate  $f(x)$  in the space  $L^2(\Omega_1) \otimes \dots \otimes L^2(\Omega_d)$  with the rank being not greater than  $p$ . Due to the low-rank structure, we will find that the polynomial mapping acting on the TNN and its derivatives can be integrated with small scale computational work. In order to show the validity of solving partial differential equations by the TNN, we introduce the following approximation result to the functions of the space  $L^2(\Omega_1 \times \dots \times \Omega_d)$  in the sense of  $L^2$ -norm.

**Theorem 1.** Assume that each  $\Omega_i$  is a bounded closed interval in  $\mathbb{R}$  for  $i = 1, \dots, d$ ,  $\Omega = \Omega_1 \times \dots \times \Omega_d$ , and the function  $f(x) \in H^m(\Omega)$ . Then for any tolerance  $\varepsilon > 0$ , there exist a positive integer  $p$  and the corresponding TNN defined by (2) such that the following approximation property holds

$$\|f(x) - \Psi(x; \theta)\|_{H^m(\Omega)} < \varepsilon. \quad (3)$$

*Proof.* Due to the isomorphism relation  $H^m(\Omega) \cong H^m(\Omega_1) \otimes \dots \otimes H^m(\Omega_d)$ , for any  $\varepsilon > 0$ , there exist a positive integer  $p$ ,  $h_{i,j}(x_i) \in H^m(\Omega_i)$ ,  $i = 1, \dots, d$ ,  $j = 1, \dots, p$ , and  $h(x) \in H^m(\Omega)$  which is defined as follows

$$h(x) = \sum_{j=1}^p h_{1,j}(x_1) \cdots h_{d,j}(x_d) = \sum_{j=1}^p \prod_{i=1}^d h_{i,j}(x_i), \quad (4)$$

such that the following estimate holds

$$\|f(x) - h(x)\|_{H^m(\Omega)} < \frac{\varepsilon}{2}. \quad (5)$$

Denote  $M_j = \max_i \|h_{i,j}(x_i)\|_{H^m(\Omega_i)}$ ,  $j = 1, \dots, p$ , and

$$M = \sum_{j=1}^p \left( \binom{d}{1} M_j^{d-1} + \binom{d}{2} M_j^{d-2} + \dots + \binom{d}{d-1} M_j^1 + 1 \right). \quad (6)$$

Since the universal approximation theorems of FNN [10, 11] can be generalized from  $\mathbb{R} \rightarrow \mathbb{R}$  to  $\mathbb{R} \rightarrow \mathbb{R}^p$  and  $C^m(\Omega_i)$  is dense in  $H^m(\Omega_i)$ , for  $\delta = \min\{1, \frac{\varepsilon}{2M}\}$ , there exist FNN structures  $\phi_i(x_i; \theta_i)$ ,  $i = 1, \dots, d$ ,  $j = 1, \dots, p$  which are defined by (1), such that

$$\|h_{i,j}(x_i) - \phi_{i,j}(x_i; \theta_i)\|_{L^2(\Omega_i)} < \delta, \quad i = 1, \dots, d, \quad j = 1, \dots, p. \quad (7)$$

Denote  $e_{i,j}(x_i) = \phi_{i,j}(x_i; \theta_i) - h_{i,j}(x_i)$ , (7) implies that  $\|e_{i,j}(x_i)\|_{H^m(\Omega_i)} < \delta$ .

Since the property of multiple integrations on the tensor product domain  $\Omega$ , for any  $g_i(x_i) \in H^m(\Omega_i)$ ,  $i = 1, \dots, d$ , the following equality holds

$$\left\| \prod_{i=1}^d g_i(x_i) \right\|_{H^m(\Omega)} \leq \prod_{i=1}^d \|g_i(x_i)\|_{H^m(\Omega_i)}. \quad (8)$$

For the sake of clarity, we give a simple proof of (8):

$$\begin{aligned} \left\| \prod_{i=1}^d g_i(x_i) \right\|_{H^m(\Omega)}^2 &= \sum_{|\alpha| \leq m} \left\| \partial^\alpha \left( \prod_{i=1}^d g_i(x_i) \right) \right\|_{L^2(\Omega)}^2 = \sum_{\alpha_1 + \dots + \alpha_d \leq m} \left\| \prod_{i=1}^d \frac{\partial^{\alpha_i} g_i(x_i)}{\partial x_i^{\alpha_i}} \right\|_{L^2(\Omega_i)}^2 \\ &= \sum_{\alpha_1 + \dots + \alpha_d \leq m} \prod_{i=1}^d \left\| \frac{\partial^{\alpha_i} g_i(x_i)}{\partial x_i^{\alpha_i}} \right\|_{L^2(\Omega_i)}^2 \leq \prod_{i=1}^d \left( \sum_{\alpha_i \leq m} \left\| \frac{\partial^{\alpha_i} g_i(x_i)}{\partial x_i^{\alpha_i}} \right\|_{L^2(\Omega_i)}^2 \right) \\ &= \prod_{i=1}^d \|g_i(x_i)\|_{H^m(\Omega_i)}^2. \end{aligned}$$

Then from the property of binomial multiplication and the equality (8), we can build a TNN  $\Psi(x; \theta)$  by (2) such that the following inequalities hold

$$\begin{aligned}
& \|h(x) - \Psi(x; \theta)\|_{H^m(\Omega)} \\
&= \left\| \sum_{j=1}^p \prod_{i=1}^d h_{i,j}(x_i) - \sum_{j=1}^p \prod_{i=1}^d (h_{i,j}(x_i) + e_{i,j}(x_i)) \right\|_{H^m(\Omega)} \\
&\leq \sum_{j=1}^p \left\| \prod_{i=1}^d h_{i,j}(x_i) - \prod_{i=1}^d (h_{i,j}(x_i) + e_{i,j}(x_i)) \right\|_{H^m(\Omega)} \\
&\leq \sum_{j=1}^p \left( \binom{d}{1} M_j^{d-1} \delta^1 + \binom{d}{2} M_j^{d-2} \delta^2 + \dots + \binom{d}{d} M_j^0 \delta^d \right) \\
&\leq \sum_{j=1}^p \left( \binom{d}{1} M_j^{d-1} + \binom{d}{2} M_j^{d-2} + \dots + \binom{d}{d-1} M_j^1 + 1 \right) \delta \\
&\leq M\delta < \frac{\varepsilon}{2}.
\end{aligned} \tag{9}$$

Therefore, from (5), (9) and triangle inequality, we have following estimates

$$\begin{aligned}
& \|f(x) - \Psi(x; \theta)\|_{H^m(\Omega)} \\
&\leq \|f(x) - h(x)\|_{H^m(\Omega)} + \|h(x) - \Psi(x; \theta)\|_{H^m(\Omega)} < \frac{\varepsilon}{2} + \frac{\varepsilon}{2} = \varepsilon.
\end{aligned}$$

This is the desired result (3) and the proof is complete.  $\square$

**Remark 1.** *The approximation property for TNN in C-norm could be similarly obtained via the isomorphism  $C(\Omega_1 \times \dots \times \Omega_d) = C(\Omega_1) \hat{\otimes}_\varepsilon \dots \hat{\otimes}_\varepsilon C(\Omega_d)$  where  $\hat{\otimes}_\varepsilon$  is the injective tensor product. The detail definition of the injective tensor product and other information can be found in [24].*

### 3 Quadrature scheme for TNN

In this section, we focus on the numerical integration of polynomial composite function of TNN and its derivatives. Our main theorem shows that the application of TNN can bring a significant reduction of the computational complexity for the related numerical integration. For convenience, we first introduce the following sets of multiple indices

$$\mathcal{B} := \left\{ \beta = (\beta_1, \dots, \beta_d) \in \mathbb{N}_0^d \mid |\beta| := \sum_{i=1}^d \beta_i \leq m \right\}, \tag{10}$$

$$\mathcal{A} := \left\{ \alpha = (\alpha_\beta)_{\beta \in \mathcal{B}} \in \mathbb{N}_0^{|\mathcal{B}|} \mid |\alpha| := \sum_{\beta \in \mathcal{B}} \alpha_\beta \leq k \right\}, \tag{11}$$

where  $\mathbb{N}_0$  denotes the set of all the non-negative integers,  $m$  and  $k$  are two positive integers,  $|\mathcal{B}|$  and  $|\mathcal{A}|$  denote the cardinal numbers of  $\mathcal{B}$  and  $\mathcal{A}$ , respectively. In this paper, we focus on

the high-dimensional cases where  $m \ll d$  and  $k \ll d$ . Simple calculation leads to the following equations

$$|\mathcal{B}| = \sum_{j=0}^m \binom{j+d-1}{j}, \quad |\mathcal{A}| = \sum_{j=0}^k \binom{j+|\mathcal{B}|-1}{j}.$$

By further estimation, we know that the scales of magnitudes of  $|\mathcal{B}|$  and  $|\mathcal{A}|$  are  $\mathcal{O}((d+m)^m)$  and  $\mathcal{O}(((d+m)^m + k)^k)$ , respectively.

Here and after, the parameter  $\theta$  in (2) has been omitted for brevity without confusion. The activation function of TNN needs to be smooth enough such that  $\Psi(x)$  has partial derivatives up to order  $m$ . Here, we assume  $F(x)$  includes the  $k$ -degree complete polynomial of  $d$ -dimensional TNN and its partial derivatives up to order  $m$  that can be expressed as follows

$$F(x) = \sum_{\alpha \in \mathcal{A}} A_\alpha(x) \prod_{\beta \in \mathcal{B}} \left( \frac{\partial^{|\beta|} \Psi(x)}{\partial x_1^{\beta_1} \cdots \partial x_d^{\beta_d}} \right)^{\alpha_\beta}, \quad (12)$$

where the coefficient  $A_\alpha(x)$  is given by the following expansion such that the rank of  $A_\alpha(x)$  is not greater than  $q$  in the tensor product space  $L^2(\Omega_1) \otimes \cdots \otimes L^2(\Omega_d)$

$$A_\alpha(x) = \sum_{\ell=1}^q B_{1,\ell,\alpha}(x_1) B_{2,\ell,\alpha}(x_2) \cdots B_{d,\ell,\alpha}(x_d). \quad (13)$$

Here  $B_{i,\ell,\alpha}(x_i)$  denotes the one-dimensional function in  $L^2(\Omega_i)$  for  $i = 1, \dots, d$  and  $\ell = 1, \dots, q$ . When using NNs to solve PDE problems, we always need to do the high-dimensional integration  $\int_\Omega F(x) dx$ . When  $\Psi(x)$  is a FNN,  $\int_\Omega F(x) dx$  can only be treated as a direct  $d$ -dimensional numerical integration, which requires exponential scale of computational work corresponding to the dimension  $d$ . In practical applications, it is well known that the high-dimensional FNN functions can only be integrated by the Monte-Carlo method with a low accuracy. Different from FNN, we will show that the high-dimensional integration  $\int_\Omega F(x) dx$  for the TNN case can be implemented by the general numerical quadrature with the polynomial scale of computational work with respect to the dimension  $d$ . This means that the TNN can cope with the curse of dimensionality in some sense.

The key idea to reduce the computational complexity of the numerical integration  $\int_\Omega F(x) dx$  is that we can decompose the TNN function  $F(x)$  into a tensor product structure. Now, we come to introduce the detailed numerical integration method for the TNN function  $F(x)$ .

Without loss of generality, for  $i = 1, \dots, d$ , we choose  $N_i$  Gauss points  $\{x_i^{(n_i)}\}_{n_i=1}^{N_i}$  and the corresponding weights  $\{w_i^{(n_i)}\}_{n_i=1}^{N_i}$  for the  $i$ -th dimensional domain  $\Omega_i$ , and denote  $N = \max\{N_1, \dots, N_d\}$ . Introducing the index  $n = (n_1, \dots, n_d) \in \mathcal{N} := \{1, \dots, N_1\} \times \cdots \times \{1, \dots, N_d\}$ , then the tensor product Gauss points and their corresponding weights on the domain  $\Omega$  can be expressed as follows

$$\begin{aligned} \{x^{(n)}\}_{n \in \mathcal{N}} &= \{x_1^{(n_1)}\}_{n_1=1}^{N_1} \times \{x_2^{(n_2)}\}_{n_2=1}^{N_2} \times \cdots \times \{x_d^{(n_d)}\}_{n_d=1}^{N_d}, \\ \{w^{(n)}\}_{n \in \mathcal{N}} &= \left\{ \prod_{i=1}^d w_i^{(n_i)} \mid w_i^{(n_i)} \in \{w_i^{(n_i)}\}_{n_i=1}^{N_i}, i = 1, \dots, d \right\}. \end{aligned} \quad (14)$$

In order to implement the decomposition, for each  $\alpha \in \mathcal{A}$ , we give the following definition

$$\mathcal{B}_\alpha := \left\{ \beta = (\beta_1, \dots, \beta_d) \in \mathcal{B} \mid \alpha_\beta \geq 1 \right\}. \quad (15)$$

By the definition of the index set  $\mathcal{A}$ , we can deduce that  $|\mathcal{B}_\alpha| \leq k$  for any  $\alpha \in \mathcal{A}$ . Then from (12) and (13), the numerical integration  $\int_\Omega F(x)dx$  can be written as follows:

$$\int_\Omega F(x)dx \approx \sum_{n \in \mathcal{N}} w^{(n)} \sum_{\alpha \in \mathcal{A}} \left( \sum_{\ell=1}^q B_{1,\ell,\alpha}(x_1^{(n_1)}) \cdots B_{d,\ell,\alpha}(x_d^{(n_d)}) \right) \prod_{\beta \in \mathcal{B}_\alpha} \left( \frac{\partial^{|\beta|} \Psi(x^{(n)})}{\partial x_1^{\beta_1} \cdots \partial x_d^{\beta_d}} \right)^{\alpha_\beta}. \quad (16)$$

Since  $\Psi(x)$  has the TNN structure (2), the cumprod can be further decomposed as

$$\begin{aligned} \prod_{\beta \in \mathcal{B}_\alpha} \left( \frac{\partial^{|\beta|} \Psi(x^{(n)})}{\partial x_1^{\beta_1} \cdots \partial x_d^{\beta_d}} \right)^{\alpha_\beta} &= \prod_{\beta \in \mathcal{B}_\alpha} \left( \frac{\partial^{|\beta|} \sum_{j=1}^p \phi_{1,j}(x_1^{(n_1)}) \cdots \phi_{d,j}(x_d^{(n_d)})}{\partial x_1^{\beta_1} \cdots \partial x_d^{\beta_d}} \right)^{\alpha_\beta} \\ &= \prod_{\beta \in \mathcal{B}_\alpha} \left( \sum_{j=1}^p \frac{\partial^{\beta_1} \phi_{1,j}(x_1^{(n_1)})}{\partial x_1^{\beta_1}} \cdots \frac{\partial^{\beta_d} \phi_{d,j}(x_d^{(n_d)})}{\partial x_d^{\beta_d}} \right)^{\alpha_\beta} \\ &= \prod_{\beta \in \mathcal{B}_\alpha} \sum_{1 \leq j_1, \dots, j_{\alpha_\beta} \leq p} \left( \frac{\partial^{\beta_1} \phi_{1,j_1}(x_1^{(n_1)})}{\partial x_1^{\beta_1}} \cdots \frac{\partial^{\beta_1} \phi_{1,j_{\alpha_1(\beta)}}(x_1^{(n_1)})}{\partial x_1^{\beta_1}} \right) \\ &\quad \cdots \left( \frac{\partial^{\beta_d} \phi_{d,j_1}(x_d^{(n_d)})}{\partial x_d^{\beta_d}} \cdots \frac{\partial^{\beta_d} \phi_{d,j_{\alpha_d(\beta)}}(x_d^{(n_d)})}{\partial x_d^{\beta_d}} \right) \\ &= \prod_{\beta \in \mathcal{B}_\alpha} \sum_{1 \leq j_1, \dots, j_{\alpha_\beta} \leq p} \left( \prod_{\ell=1}^{\alpha_\beta} \frac{\partial^{\beta_1} \phi_{1,j_\ell}(x_1^{(n_1)})}{\partial x_1^{\beta_1}} \right) \cdots \left( \prod_{\ell=1}^{\alpha_\beta} \frac{\partial^{\beta_d} \phi_{d,j_\ell}(x_d^{(n_d)})}{\partial x_d^{\beta_d}} \right) \\ &= \sum_{\substack{1 \leq j_\beta, \ell \leq p, \\ \beta \in \mathcal{B}_\alpha, \ell=1, \dots, \alpha_\beta}} \left( \prod_{\beta \in \mathcal{B}_\alpha} \prod_{\ell=1}^{\alpha_\beta} \frac{\partial^{\beta_1} \phi_{1,j_\beta,\ell}(x_1^{(n_1)})}{\partial x_1^{\beta_1}} \right) \cdots \left( \prod_{\beta \in \mathcal{B}_\alpha} \prod_{\ell=1}^{\alpha_\beta} \frac{\partial^{\beta_d} \phi_{d,j_\beta,\ell}(x_d^{(n_d)})}{\partial x_d^{\beta_d}} \right). \quad (17) \end{aligned}$$

With the help of expansion (17), we can give the following numerical integration scheme for  $\int_\Omega F(x)dx$ :

$$\begin{aligned} \int_\Omega F(x)dx &\approx \sum_{n_1=1}^{N_1} \cdots \sum_{n_d=1}^{N_d} w_1^{(n_1)} \cdots w_d^{(n_d)} \sum_{\alpha \in \mathcal{A}} \left( \sum_{\ell=1}^q B_{1,\ell,\alpha}(x_1^{(n_1)}) \cdots B_{d,\ell,\alpha}(x_d^{(n_d)}) \right) \\ &\quad \cdot \sum_{\substack{1 \leq j_\beta, \ell \leq p, \\ \beta \in \mathcal{B}_\alpha, \ell=1, \dots, \alpha_\beta}} \left( \prod_{\beta \in \mathcal{B}_\alpha} \prod_{\ell=1}^{\alpha_\beta} \frac{\partial^{\beta_1} \phi_{1,j_\beta,\ell}(x_1^{(n_1)})}{\partial x_1^{\beta_1}} \right) \cdots \left( \prod_{\beta \in \mathcal{B}_\alpha} \prod_{\ell=1}^{\alpha_\beta} \frac{\partial^{\beta_d} \phi_{d,j_\beta,\ell}(x_d^{(n_d)})}{\partial x_d^{\beta_d}} \right) \\ &= \sum_{\alpha \in \mathcal{A}} \sum_{\ell=1}^q \sum_{\substack{1 \leq j_\beta, \ell \leq p, \\ \beta \in \mathcal{B}_\alpha, \ell=1, \dots, \alpha_\beta}} \left( \sum_{n_1=1}^{N_1} w_1^{(n_1)} B_{1,\ell,\alpha}(x_1^{(n_1)}) \prod_{\beta \in \mathcal{B}_\alpha} \prod_{\ell=1}^{\alpha_\beta} \frac{\partial^{\beta_1} \phi_{1,j_\beta,\ell}(x_1^{(n_1)})}{\partial x_1^{\beta_1}} \right) \\ &\quad \cdots \left( \sum_{n_d=1}^{N_d} w_d^{(n_d)} B_{d,\ell,\alpha}(x_d^{(n_d)}) \prod_{\beta \in \mathcal{B}_\alpha} \prod_{\ell=1}^{\alpha_\beta} \frac{\partial^{\beta_d} \phi_{d,j_\beta,\ell}(x_d^{(n_d)})}{\partial x_d^{\beta_d}} \right). \quad (18) \end{aligned}$$

The quadrature scheme (18) decomposes the high-dimensional integration  $\int_\Omega F(x)dx$  into to a series of one-dimensional integration. Due to the simplicity of the one-dimensional integration, the scheme

(18) can reduce the computational work of the high-dimensional integration for the  $d$ -dimensional function  $F(x)$  to the polynomial scale of dimension  $d$ .

**Theorem 2.** *Assume that the function  $F(x)$  is defined as (12), where the coefficient  $A_\alpha(x)$  has the expansion (13). On the  $d$ -dimensional tensor product domain  $\Omega$ , we choose the tensor product Gauss points and their corresponding weights which are defined by (14) to determine the quadrature scheme. Based on these Gauss points and weights, let us perform the numerical integration (18) for the function  $F(x)$  on the domain  $\Omega$ . Let  $T_1$  denote the computational complexity for the 1-dimensional function evaluation operations.*

*If the function  $\Psi(x)$  involved in the function  $F(x)$  has the TNN form (2), the computational complexity for the numerical integration (18) can be bounded by  $\mathcal{O}(dqT_1k^2p^k((d+m)^m+k)^kN)$ , which is the polynomial scale of the dimension  $d$ .*

*Proof.* First, we show that the number of  $j_{\beta,\ell}$  in the last summation of (17) is no more than  $k$ . This result can be easily proved by the following inequality

$$\sum_{\beta \in \mathcal{B}_\alpha} \alpha_\beta = |\alpha| \leq k. \quad (19)$$

Then, by direct calculation, the computational complexity of (18) can be bounded by  $\mathcal{O}(dqT_1k^2p^k((d+m)^m+k)^kN)$ . This is the desired result and the proof is complete.  $\square$

If  $\Psi(x)$  does not have the tensor form, it is easy to know that the computational complexity for the functions defined by the NN is  $\mathcal{O}((dqT_1+kT_d)((d+m)^m+k)^kN^d)$ , where  $T_d$  denotes the complexity for the  $d$ -dimensional function evaluation operations.

## 4 Solving high-dimensional eigenvalue problem by TNN

This section is devoted to discussing the application of TNNs to the numerical solution of the high-dimensional second order elliptic eigenvalue problem. For simplicity, we are concerned with the following model problem:

$$\begin{cases} -\Delta u + vu = \lambda u, & \text{in } \Omega, \\ u = 0, & \text{on } \partial\Omega, \end{cases} \quad (20)$$

where  $\Omega = \Omega_1 \times \cdots \times \Omega_d$ , each  $\Omega_i = (a_i, b_i)$ ,  $i = 1, \dots, d$  is a bounded interval in  $\mathbb{R}$ ,  $v \in L^2(\Omega)$  is a potential function. We assume that the rank of  $v$  is finite in the tensor product space  $L^2(\Omega_1) \otimes \cdots \otimes L^2(\Omega_d)$ . The potential function  $v$  often occurs in quantum mechanics problems. In this paper, we consider the zero function

$$v(x) = 0, \quad \text{in } \Omega, \quad (21)$$

and the harmonic oscillator

$$v(x) = \sum_{i=1}^d x_i^2, \quad \text{in } \Omega. \quad (22)$$



In quantum mechanics, the eigenvalue problem (20) with the potential function (21) is the Schrödinger equation with infinite potential well. The eigenvalue problem with the potential (22) comes from the truncation of the Schrödinger equation with the harmonic oscillator potential which is defined in the whole space.

There is a well-known variational principle or minimum theorem of the problem (20) for the smallest eigenpair  $(\lambda, u)$ :

$$\lambda = \min_{w \in H_0^1(\Omega)} \mathcal{R}(w) = \min_{w \in H_0^1(\Omega)} \frac{\int_{\Omega} |\nabla w|^2 dx + \int_{\Omega} v w^2 dx}{\int_{\Omega} w^2 dx}, \quad (23)$$

where  $\mathcal{R}(w)$  denotes the Rayleigh quotient for the function  $w \in H_0^1(\Omega)$ .

In order to solve the eigenvalue problem (20), we build a TNN structure  $\Psi(x; \theta)$  which is defined by (2), and define the set of all possible values of  $\theta$  as  $\Theta$ . In order to avoid the penalty on boundary condition, we simply use the method in [8] to treat the Dirichlet boundary condition. This method is firstly proposed in [18, 19]. For  $i = 1, \dots, d$ , the  $i$ -th subnetwork  $\phi_i(x_i; \theta_i)$  is defined as follows:

$$\begin{aligned} \phi_i(x_i; \theta_i) &:= (x_i - a_i)(b_i - x_i) \widehat{\phi}_i(x_i; \theta_i) \\ &= \left( (x_i - a_i)(b_i - x_i) \widehat{\phi}_{i,1}(x_i; \theta_i), \dots, (x_i - a_i)(b_i - x_i) \widehat{\phi}_{i,d}(x_i; \theta_i) \right)^T, \end{aligned} \quad (24)$$

where  $\widehat{\phi}_i(x_i; \theta_i)$  is a FNN from  $\mathbb{R}$  to  $\mathbb{R}^p$  with sufficient smooth activation functions, such that  $\Psi(x; \theta) \in H_0^1(\Omega)$ .

The trial function set  $V$  is modeled by the TNN structure  $\Psi(x; \theta)$  where parameters  $\theta$  take all the possible values and it is obvious that  $V \subset H_0^1(\Omega)$ . The solution and the parameters  $(\lambda^*, \Psi(x; \theta^*))$  of the following optimization problem are approximations to the smallest eigenpair:

$$\lambda^* = \min_{\Psi(x; \theta) \in V} \mathcal{R}(\Psi(x; \theta)) = \min_{\theta \in \Theta} \frac{\int_{\Omega} |\nabla \Psi(x; \theta)|^2 dx + \int_{\Omega} v(x) \Psi^2(x; \theta) dx}{\int_{\Omega} \Psi^2(x; \theta) dx} = \mathcal{R}(\Psi(x; \theta^*)). \quad (25)$$

Note that all integrands of the numerator and the denominator of (25) have the form (12). With the help of Theorem 2, we can implement these numerical integration by scheme (18) with the computational work being bounded by the polynomial scale of dimension  $d$ . We choose the tensor product Gauss points and their corresponding weights which are defined by (14) to discretize these integrations, and define the loss function as follows:

$$L(\theta) := \frac{\sum_{n \in \mathcal{N}} w^{(n)} |\nabla \Psi(x^{(n)}, \theta)|^2 + \sum_{n \in \mathcal{N}} w^{(n)} v(x^{(n)}) \Psi^2(x^{(n)}; \theta)}{\sum_{n \in \mathcal{N}} \Psi^2(x^{(n)}; \theta)}. \quad (26)$$

In this paper, the gradient descent (GD) method is adopted to minimize the loss function  $L(\theta)$ . The GD scheme can be described as follows:

$$\theta^{(k+1)} = \theta^{(k)} - \eta \nabla L(\theta^{(k)}), \quad (27)$$

where  $\theta^{(k)}$  denotes the parameters after the  $k$ -th gradient descent step,  $\eta$  is the learning rate (step size).

Different from the general FNN-based machine learning method, we use the fixed quadrature points  $\{x^{(n)}\}_{n \in \mathcal{N}}$  to do the numerical integration in this paper. Using the fixed quadrature points for FNN, the computational work for the numerical integration will depend exponentially on the dimension  $d$ . In order to avoid the ‘‘curse of dimensionality’’, in the numerical implementation for solving the high-dimensional PDEs by FNN-based method, the stochastic gradient descent (SGD) method [16] with Monte Carlo integration are always used [5]. The application of random sampling quadrature points always leads to the low accuracy and instability convergence for the FNN method.

Fortunately, based on TNN structure in the loss function (26), Theorem 2 shows that the numerical integration does not encounter ‘‘curse of dimensionality’’ since the computational work can be bounded by the polynomial scale of dimension  $d$ . This is the reason we can use GD method to solve the optimization problem (25) instead of SGD in this paper. That is to say, using all quadrature points to implement the integration and then the GD step (27) in TNN-based machine learning are reasonable. Due to the high accuracy of the tensor product with Gauss points and Theorem 1, the high accuracy of the TNN-based method can be guaranteed.

## 5 Numerical results

In this section, we provide several examples to validate the efficiency and accuracy of the TNN-based machine learning method proposed in this paper. To demonstrate the capability and accuracy of TNN, we solve the high-dimensional second order elliptic eigenvalue problems (20).

In each example we will check the performances of TNN for three cases of dimensions:  $d = 128$ ,  $d = 256$  and  $d = 512$ . The solution  $u(x)$  is approximated by a TNN structure  $\Psi(x; \theta)$  which is defined by (2). Each subnetwork in  $\Psi(x; \theta)$  is a FNN which is defined by (1) with 2 hidden layers and 10 hidden nodes per layer. Let  $p = 5$  in all cases. Then the number of trainable parameters of  $\Psi(x; \theta)$  is  $160d$ . Here, we choose the hyperbolic tangent function  $\tanh(x)$  as the activation function.

In order to show the convergence behavior and accuracy of eigenfunction approximations by TNN, we define the  $L^2(\Omega)$  projection operators  $\mathcal{P} : H_0^1(\Omega) \rightarrow \text{span}\{\Psi(x; \theta^*)\}$  as follows:

$$\langle \mathcal{P}u, v \rangle_{L^2} = \langle u, v \rangle_{L^2} := \int_{\Omega} uv dx, \quad \forall v \in \text{span}\{\Psi(x; \theta^*)\} \text{ for } u \in H_0^1(\Omega). \quad (28)$$

And we define the  $H^1(\Omega)$  projection operators  $\mathcal{Q} : H_0^1(\Omega) \rightarrow \text{span}\{\Psi(x; \theta^*)\}$  as follows:

$$\langle \mathcal{Q}u, v \rangle_{H^1} = \langle u, v \rangle_{H^1} := \int_{\Omega} \nabla u \cdot \nabla v dx, \quad \forall v \in \text{span}\{\Psi(x; \theta^*)\} \text{ for } u \in H_0^1(\Omega). \quad (29)$$

Then we define the following errors for the approximated eigenvalue  $\lambda^*$  and eigenfunction  $\Psi(x; \theta^*)$

$$e_{\lambda} := \frac{|\lambda^* - \lambda|}{|\lambda|}, \quad e_{L^2} := \frac{\|u - \mathcal{P}u\|_{L^2(\Omega)}}{\|u\|_{L^2(\Omega)}}, \quad e_{H^1} := \frac{|u - \mathcal{Q}u|_{H^1(\Omega)}}{|u|_{H^1(\Omega)}}, \quad (30)$$

in all examples. Here  $\|\cdot\|_{L^2}$  and  $|\cdot|_{H^1}$  denote  $L^2(\Omega)$  norm and  $H^1(\Omega)$  seminorm, respectively. These relative errors are often used to test numerical methods for eigenvalue problems. Since the rank of the exact solution  $u(x)$  in each example is finite in the tensor product space  $L^2(\Omega_1) \otimes \cdots \otimes L^2(\Omega_d)$ ,

all integrations in the numerators and denominators of the  $L^2(\Omega)$  relative error  $e_{L^2}$  and the  $H^1(\Omega)$  relative error  $e_{H^1}$  have the form (12). When computing  $e_{L^2}$  and  $e_{H^1}$ , we also use the numerical integration scheme (18) with the same tensor product Gauss points and weights as computing the loss functions. With the help of Theorem 2 and the Gauss quadrature points, the high efficiency and accuracy in computing  $e_{L^2}$  and  $e_{H^1}$  can be guaranteed.

To implement the GD method, we use all quadrature points and weights to construct the loss function as (26), and train the networks by Adam optimizer [16]. The Adam optimizer does not randomly choose the data points for computing the loss functions. The only reason to use Adam optimizer is that it can compute individual adaptive learning rates for different parameters.

### 5.1 Laplace eigenvalue problem

In the first example, the potential function is defined as (21) with the domain  $\Omega = \Omega_1 \times \dots \times \Omega_d$ ,  $\Omega_i = (0, 1)$  for  $i = 1, \dots, d$ . Then the exact smallest eigenvalue and eigenfunction are

$$\lambda = d\pi^2, \quad u(x) = \prod_{i=1}^d \sin(\pi x_i). \quad (31)$$

Here, in order to compute the loss function  $L(\theta)$  and relative errors  $e_{L^2}$  and  $e_{H^1}$ , we decompose  $\Omega_i$  ( $i = 1, \dots, d$ ) into 10 equal subintervals and choose 4 Gauss points on each subinterval. The Adam optimizer is employed to train the TNN with learning rate 0.0001. Figure 1 shows the relative errors  $e_\lambda$ ,  $e_{L^2}$  and  $e_{H^1}$  versus the number of epochs. The final relative errors after 50,000 epochs are reported in Table 1 for different dimensional cases.

Table 1: Errors of Laplace eigenvalue problem for  $d = 128, 256, 512$ .

$d$	$e_\lambda$	$e_{L^2}$	$e_{H^1}$
128	1.674e-07	1.041e-03	1.118e-03
256	1.497e-07	1.484e-03	1.534e-03
512	1.629e-07	2.500e-03	2.532e-03

From Figure 1 and Table 1, we can find that the TNN method has almost the same convergence behaviors for different dimensions. The numerical results also show that the accuracy of TNN is better than FNN-based machine learning method [5].

### 5.2 Eigenvalue problem with harmonic oscillator

In the second example, the potential function is defined as (22). Then the exact smallest eigenvalue and eigenfunction are

$$\lambda = d, \quad u(x) = \prod_{i=1}^d e^{-x_i^2/2}. \quad (32)$$

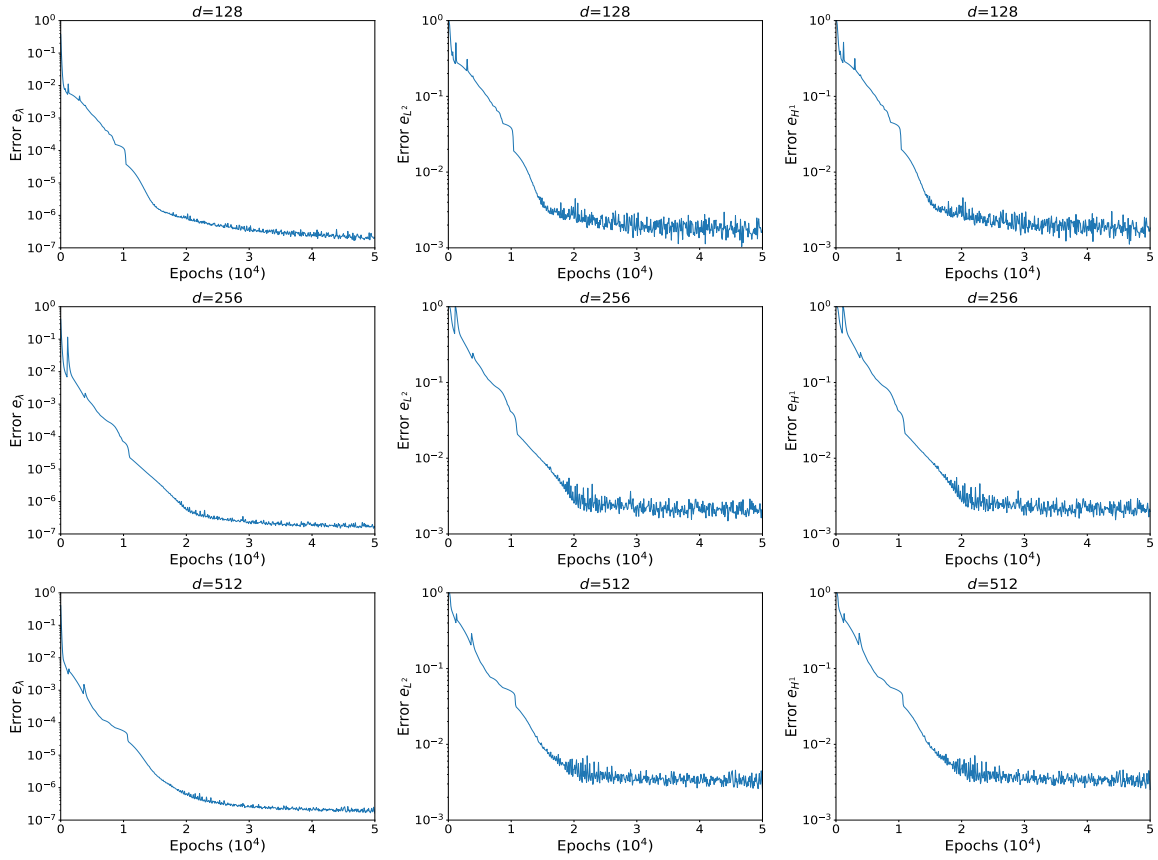


Figure 1: Relative errors during the training process for Laplace eigenvalue problem: for  $d = 128$ , 256 and 512. The left column shows the relative errors of eigenvalue approximations, the middle column shows the relative  $L^2(\Omega)$  errors and the right column shows the relative  $H^1(\Omega)$  errors.

We truncate the computational domain to  $\Omega = \Omega_1 \times \cdots \times \Omega_d$ , where  $\Omega_i = (-5, 5)$  for  $i = 1, \dots, d$ . In order to compute the loss function  $L(\theta)$  and relative errors  $e_{L^2}$  and  $e_{H^1}$ , we decompose  $\Omega_i$  ( $i = 1, \dots, d$ ) into 50 subintervals and choose 4 Gauss Points on each subinterval. The Adam optimizer is also employed to train the TNN with learning rate 0.001. Figure 2 shows the relative errors  $e_\lambda$ ,  $e_{L^2}$  and  $e_{H^1}$  versus the number of epochs. The final relative errors after 50,000 epochs are reported in Table 2 for different dimensional cases.

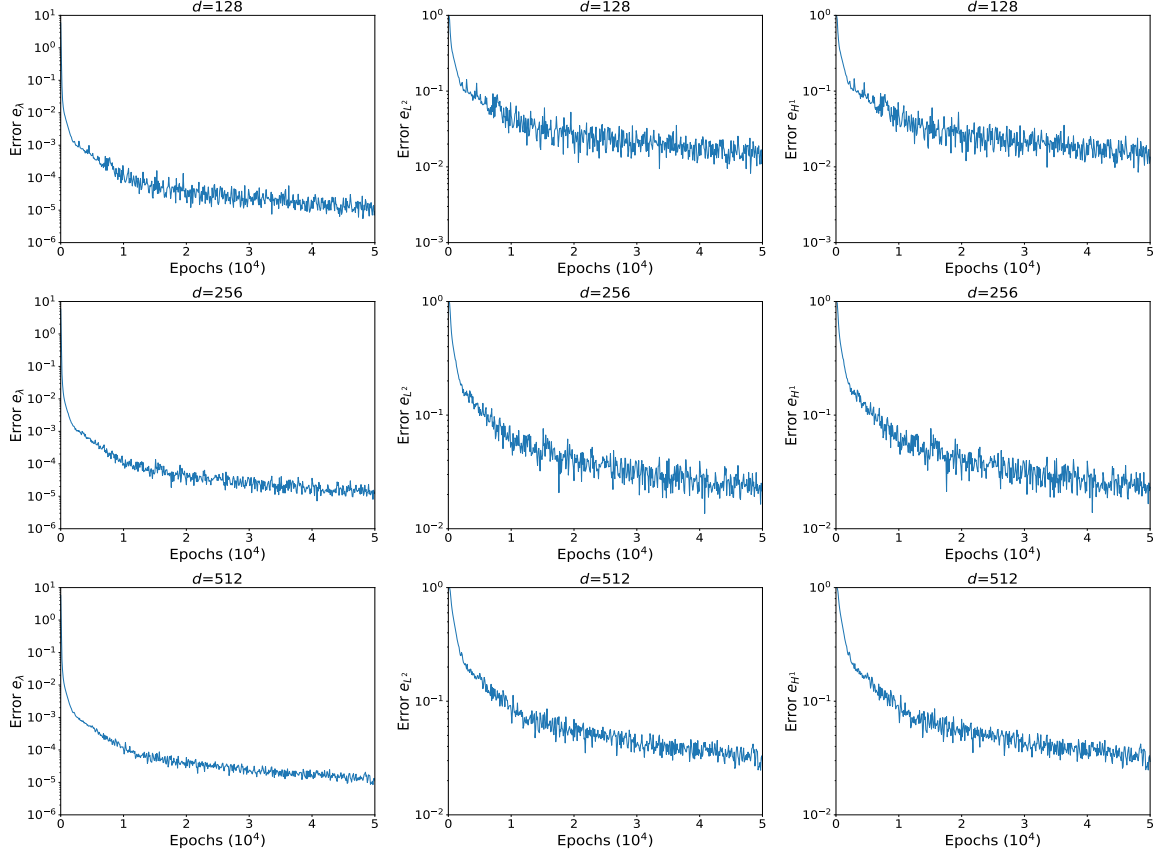


Figure 2: Relative errors during the training process for the harmonic oscillator problem: for  $d = 128, 256, 512$ . The left column shows the relative errors of eigenvalue, the middle column shows the relative  $L^2$  errors and the right column shows the relative  $H^1$  errors.

Table 2: Errors of the harmonic oscillator problem for  $d = 128, 256, 512$ .

$d$	$e_\lambda$	$e_{L^2}$	$e_{H^1}$
128	5.483e-06	8.221e-03	8.500e-03
256	7.166e-06	1.362e-02	1.387e-02
512	8.530e-06	2.471e-02	2.480e-02

Figure 2 and Table 2 also show that the dimension has less effect on the convergence behaviors

of TNN method. From Figure 2, we can also find that the errors still have the decreasing trend after 50000 epochs. There should exist some room for improving the accuracy.

## 6 Conclusions

In this paper, we present the TNN and corresponding machine learning method. Different from the general FNN-based machine learning method, TNN decomposes the NN into the tensor product form and its numerical integration uses the fixed quadrature points in each dimension. Benefit from the tensor product structure, we can design an efficient integration scheme for the functions defined based on TNN. These properties lead to the TNN-based machine learning which can deal with the direct inner product computation with the polynomial scale of work with respect to the dimension. We believe that the ability of direct inner production computation will bring more applications in solving high-dimensional PDEs.

Based on the ideas of CP decomposition for tensor product Hilbert space and representing the trial functions by deep neural networks, we introduce a type of TNN structure and the corresponding approximation property, and efficient numerical integration scheme are also presented. The theoretical results, algorithms and numerical experiments show that this type of structure have following advantages:

1. With the help of the tensor product representation way, we can treat this type of functions separately in one-dimensional interval. This is the reason to overcome the exponential dependence of the computational work on the dimension.
2. Instead of randomly sampling data points, the data points used in the training process are fixed quadrature points. This means that the TNN method can avoid the randomly sampling process to produce the GD direction in each step. Then the TNN method has better stability.

Besides above remarks, there should be some interesting directions that need to be addressed in future work:

1. The choice of the subnetwork structure, the activation function and more important hyperparameter  $p$ .
2. When the computing domain is not tensor-product type, further strategies are needed to maintain the high efficiency and accuracy of the numerical integration.
3. Since TNN uses the fixed quadrature points, we should design more efficient optimization methods for the included optimization problem in the machine learning process.

In addition, more applications to other types of problems should be considered in future.

## References

- [1] M. Baymani, S. Effati, H. Niazmand and A. Kerayechian, Artificial neural network method for solving the Navier-Stokes equations. *Neural Comput & Applic.*, 26(4) (2015), 765–763.
- [2] G. Beylkin and M. J. Mohlenkamp, Numerical operator calculus in higher dimensions. *Proceedings of the National Academy of Sciences*, 99(16): 10246–10251, 2002.
- [3] G. Beylkin and M. J. Mohlenkamp, Algorithms for numerical analysis in high dimensions. *SIAM Journal on Scientific Computing*, 26(6) (2005), 2133–2159.
- [4] W. E, Machine learning and computational mathematics. *Commun. Comput. Phys.*, 28 (2020), 1639–1670.
- [5] W. E and B. Yu, The Deep Ritz Method: a deep-learning based numerical algorithm for solving variational problems. *Commun. Math. Stat.*, 6 (2018), 1–12.
- [6] X. Glorot and Y. Bengio, Understanding the difficulty of training deep feedforward neural networks. In *Proceedings of the thirteenth international conference on artificial intelligence and statistics*, 249–256, 2010.
- [7] I. Goodfellow, Y. Bengio and A. Courville, *Deep Learning*. MIT Press, Cambridge, 2016.
- [8] Y. Gu, C. Wang and H. Yang, Structure probing neural network deflation. *Journal of Computational Physics*, 434 (2021), 110231.
- [9] J. H. Halton, on the efficiency of certain quasi-random sequences of points in evaluating multidimensional integrals. *Numer. Math.*, 2 (1960), 84–90.
- [10] K. Hornik, M. Stinchcombe, H. White. Multilayer feedforward networks are universal approximators. *Neural networks*, 2(5) (1989), 359-366.
- [11] K. Hornik, M. Stinchcombe and H. White. Universal approximation of an unknown mapping and its derivatives using multilayer feedforward networks. *Neural networks*, 1990, 3(5): 551-560.
- [12] W. Hackbusch, B. N. Khoromskij, Tensor-product approximation to operators and functions in high dimensions. *Journal of Complexity*, 23(4-6) (2007), 697–714.
- [13] J. Han, A. Jentzen and W. E, Overcoming the curse of dimensionality: Solving high-dimensional partial differential equations using deep learning. *arXiv:1707.02568v1*, 2017.
- [14] D. Hong and T. G. Kolda, and J. A. Duersch, Generalized canonical polyadic tensor decomposition. *SIAM Review*, 62(1) (2020), 133–163.
- [15] P. Jin, S. Meng, L. Lu, MIONet: Learning multiple-input operators via tensor product. *arXiv:2202.06137*, 2022.

- [16] D. P. Kingma and J. Ba, Adam: A method for stochastic optimization. arXiv:1412.6980, 2014; Published as a conference paper at ICLR 2015.
- [17] T. G. Kolda and B. W. Bader, Tensor decompositions and applications. *SIAM Review*, 51(3) (2009), 455–500.
- [18] I. E. Lagaris, A. Likas, and D. I. Fotiadis, Artificial neural networks for solving ordinary and partial differential equations. *IEEE Transactions on Neural Networks*, 9 (1998), 987–1000.
- [19] I. E. Lagaris, A. C. Likas, and G. D. Papageorgiou, Neural-network methods for boundary value problems with irregular boundaries. *IEEE Transactions on Neural Networks*, 11 (2000), 1041–1049.
- [20] M. S. Litsarev and I. V. Oseledets, Fast low-rank approximations of multidimensional integrals in ion-atomic collisions modelling. *Numerical Linear Algebra with Applications*, 22(6) (2015), 1147–1160.
- [21] J. Nocedal and S. Wright, *Numerical optimization*. Springer Science & Business Media, 2006.
- [22] M. Raissi, P. Perdikaris and G. E. Karniadakis, Physics informed deep learning (part I): Data-driven solutions of nonlinear partial differential equations. arXiv:1711.10561, 2017.
- [23] M. J. Reynolds, A. Doostan, and G. Beylkin, Randomized alternating least squares for canonical tensor decompositions: Application to a PDE with random data. *SIAM Journal on Scientific Computing*, 38(5): A2634–A2664, 2016.
- [24] R. A. Ryan, *Introduction to tensor products of Banach spaces*. London: Springer, 2002.
- [25] J. Sirignano and K. Spiliopoulos, DGM: A deep learning algorithm for solving partial differential equations. *Journal of Computational Physics*, 375 (2018), 1339–1364.